Proceedings of the LHCP2015 Conference, St. Petersburg, Russia, August 31 - September 5, 2015

Editors: V.T. Kim and D.E. Sosnov

Search for Quantum Black Holes in Lepton+Jet Final State Using pp-Collisions at $\sqrt{s}$ = 8 TeV with the ATLAS

Z.M. KARPOVA[1,a)] S.N. KARPOV[1,b)]

[1] *Joint Institute for Nuclear Research, Dubna*

[a)]Corresponding author: zkarpova@cern.ch
[b)]skarpov@cern.ch

On behalf of the ATLAS Collaboration

Abstract. Search for quantum black holes (QBHs) was performed with proton-proton collision data collected by the ATLAS detector at the LHC in 2012 at a center-of-mass energy $\sqrt{s}$ = 8 TeV with the integrated luminosity of 20.3 fb^{-1}. The QBH production is modeled with the ADD-model with the number of large extra dimensions n = 6. The QBH is assumed to decay into a final state with a lepton (electron or muon) and a jet. This final state is preferred in the above model and it is assumed to be sensitive to the TeV scale gravity. There are no events with a lepton-jet invariant mass of 3.5 TeV or more in both electron and muon channel. The measurement is consistent with the expected background. The combined 95% confidence level upper limit on product of the QBH production cross sections and the branching fractions of decay into the lepton+jet is equal to 0.18 fb. The upper limit constrains the threshold quantum black-hole mass to be above 5.3 TeV in the model considered.

INTRODUCTION

This paper presents a search for Quantum Black Hole (QBH) production in pp collisions at the ATLAS detector. Analysis was done for Run 1 (2012) at a center-of-mass energy $\sqrt{s}$ = 8 TeV with the integrated luminosity of 20.3 ± 0.6 fb^{-1}. This model offers an interesting search channel to be performed at the Large Hadron Collider (LHC) because quantum black holes are predicted in low-scale quantum gravity theories which offer solutions to the mass hierarchy problem of the Standard Model (SM) by lowering the scale of quantum gravity (M_{D}) from the Planck scale ~10^{16} TeV to ~1 TeV. That is why a search region for invariant masses of QBH is studied near 1-10 TeV. Here M_{D} is a multidimensional mass of QBH.

The Large Extra Spatial Dimension Model with n compact extra dimensions with a gravitational radius R was suggested by Arkani-Hamed, Dimopoulos and Dvali (ADD-model) [1, 2, 3]. The analysis utilizes the feature of the model that the QBHs with masses near M_{D}, postulated to conserve total angular momentum, color, and electric charge, may decay to two particles [4]. The behavior of QBHs is different from semi-classical black holes that decay via Hawking radiation to a large number of objects [5]. The two-particle decay of QBH into a lepton (electron or muon) and a light quark (u or d) violates conservation of both lepton and baryon number and provides a distinctive signal for physics beyond the SM. Therefore, it is assumed in this analysis that QBHs decay mode is with one lepton (electron or muon) and a jet in final state with a high invariant mass. This mode also has the highest branching fraction and ratio of signal to background in comparison with other possible decay modes [4].

A brief description of the ADD Model

To solve the hierarchy problem the multi-dimensional Planck scale is assumed to be equal to the electroweak scale $M_{\mathrm{D}} = M_{\mathrm{EWK}}$, where the electroweak scale is M_{EWK} ~1 TeV and the true Planck scale is equal $M_{\mathrm{Pl}} \sim 10^{16}$ TeV. Therefore the gravity becomes strong, and quantum effects are important. The true Planck scale (M_{Pl}) is related to multi-dimensional one (M_{D}) as:

$$M_{\mathrm{Pl}}^2 \sim M_{\mathrm{D}}^{2+n} \cdot R^n. \quad (1)$$

Extra spatial dimensions are large, i.e. their gravitational radius R could be about 1μm or even up to ~1 mm. According to the ADD scenario it is expected, if collisions energy will exceed a certain threshold mass M_{th}, the microscopic black holes should form. The threshold mass can be above M_{D}, but far below M_{Pl}. This phenomenology of QBHs production should be significantly different from production of semi-classical black holes: if the black hole was produced far above threshold M_{th}, then it can decay into large quantity of objects via the Hawking radiation. In case of Quantum Black Hole: the QBH could form near threshold M_{th} and later it can decay into the two-body final states. The production of QBH close to M_{th} dictates a possible quasi-resonant final state with an observable enhancement for a certain invariant mass.

The largest cross section of QBH production for a final state with a lepton and a jet depends on the initial state. For the initial state with two u-quarks the QBH is produced with an electric charge of +4/3 and the branching fraction is $BF = 11\%$. For the ud-quarks collision the QBH will have charge of +1/3 and the Branching Fraction will be $BF = 5.7\%$. For the initial dd-quarks and QBH with charge of -2/3 the branching fraction is $BF = 6.7\%$. Processes with initial states of anti-quarks and heavier sea-quarks are suppressed by a factor of ~100.

THE ATLAS DETECTOR

The ATLAS detector [6] is a multipurpose detector with a forward-backward symmetric cylindrical geometry and it covers about 4π of solid angle. The dimensions of the detector are 25 m in height and 44 m in length. The overall weight of the detector is approximately 7000 tons.

Identification of vertex, electrons, muons and jets and measurement of energy and momentum are achieved by a combination of different detectors and systems. They are Magnetic system, Inner Detector, Liquid-Argon electromagnetic calorimeter, Hadronic calorimeters and Muon System. Inner Detector (tracker) covers a pseudo-rapidity range of $|\eta| < 2.5$. The pseudo-rapidity, η, is defined by equation:

$$\eta = -\log\left(\tan\frac{\theta}{2}\right). \quad (2)$$

The Inner Detector is surrounded by a superconducting solenoid providing a 2 T magnetic field in the central tracking volume with a peak field of 2.6 T. A liquid-Argon (LAr) electromagnetic (EM) sampling calorimeter provides the energy measurements in range $|\eta| < 3.2$. A scintillator-tile hadronic calorimeter (TileCal) covers range $|\eta| < 1.7$. A LAr hadronic calorimeter covers $1.4 < |\eta| < 3.2$, and a LAr forward calorimeter covers $3.1 < |\eta| < 4.9$. The Muon Spectrometer (MS) consists of tracking chambers covering $|\eta| < 2.7$ and trigger chambers covering $|\eta| < 2.4$ in a magnetic field produced by a system of air-core toroids. Magnetic field is ~0.5 T and ~1 T for the central and end-cap regions of the muon detector, respectively.

EVENT SELECTION

Six criteria of the object selection are used in the analysis [7]:

1. In the electron (muon) channel events are required to have exactly 1 electron (muon).
2. Electron candidates are identified as localized depositions of energy in the EM calorimeter with $p_{\mathrm{T}} > 130$ GeV and $|\eta| < 2.47$, excluding the barrel-endcap transition region, $1.37 < |\eta| < 1.52$, and matched to a track reconstructed in the tracking detectors.
3. Isolated electrons are selected by requiring the transverse energy deposited in a cone of radius $\Delta R = \sqrt{(\Delta\eta)^2 + (\Delta\phi)^2} = 0.3$ centered on the electron cluster, excluding the energy of the electron cluster itself, to be less than $(0.0055 \cdot p_{\mathrm{T}} + 3.5)$ GeV after corrections for energy due to pileup and energy leakage from the electron cluster into the cone.
4. Muon candidates are required to be detected in at least three layers of the muon spectrometer and to have $p_{\mathrm{T}} > 130$ GeV and $|\eta| < 2.4$.
5. Signal muons are required to be isolated such, that $\sum p_{\mathrm{T}} < 0.05 \cdot p_{\mathrm{T}\mu}$, where $\sum p_{\mathrm{T}}$ is the sum of the p_{T} of the other tracks in a cone of radius $\Delta R = 0.3$ around the direction of the muon.
6. Jets are constructed from three-dimensional noise-suppressed clusters of calorimeter cells using the anti-kt algorithm with a radius parameter of 0.4. All jets are required to have $p_{\mathrm{T}} > 50$ GeV and $|\eta| < 2.5$. In addition, the most energetic jet is required to have $p_{\mathrm{T}} > 130$ GeV.

SOURCES OF BACKGROUND FOR QUANTUM BLACK HOLES

Events with a high p_T of lepton and one or more jets can arise from electroweak processes. They include a vector-boson production with additional jets and di-bosons (WW, WZ, ZZ). Strong processes include top-quark pairs ($t\bar{t}$), a single top-quark (t or $\bar{t}$) and multi-jets (QCD) production. The multi-jets background can include non-prompt leptons from the semi-leptonic hadrons decays and also include jets, which were identified as leptons by mistake.

Multi-jets background was estimated with a data-driven method. The electroweak background and strong production of top-quarks were estimated in Signal Region using Monte Carlo samples, normalized to data in Control Regions. Simulation was based on GEANT4 [8] with the corresponding model of the ATLAS detector geometry. List of dominant backgrounds in decreasing order of importance is below:

- W+jets;
- Z+jets;
- Di-bosons: WW, WZ, ZZ;
- Production of $t\bar{t}$ pairs;
- Single top-quarks;
- Multi-jets (QCD).

Additional inelastic proton-proton's interactions, termed pileup, were included into the event simulation in order to agree with the data distribution of the number of interactions per bunch crossing. The average number of interactions per bunch crossing was about 21.

RESULTS OF THE SEARCH FOR QBH IN RUN 1

The invariant mass (m_{inv}) is calculated with two 4-vectors of the lepton and highest-p_T jet. The Signal Region (SR) is defined by a lower bound, m_{min}, of invariant mass, that accounts for experimental resolution. In the electron channel $m_{min} = 0.9 \cdot M_{th}$ is used. In the muon channel, the requirement is loosened at high invariant mass, as muon resolution has a term quadratic in p_T, resulting in $m_{min} = (0.95 - 0.05 \cdot M_{th}/1\ \text{TeV}) \cdot M_{th}$. A low invariant-mass Control Region (CR) is defined with m_{inv} between 400 and 900 GeV, which has a negligible contamination from a potential signal ($< 2\%$) for the lowest M_{th} considered.

In Figure 1 you can see the distribution of events over the invariant mass of the lepton and highest-p_T jet for data (points with error bars) and for SM backgrounds (solid histograms) [7]. Panel (a) corresponds to the electron channel and panel (b) – muon channel. The hatched area shows the total uncertainty in the background estimate, in which the systematic uncertainties dominate. Dashed lines represent two examples of QBH signals.

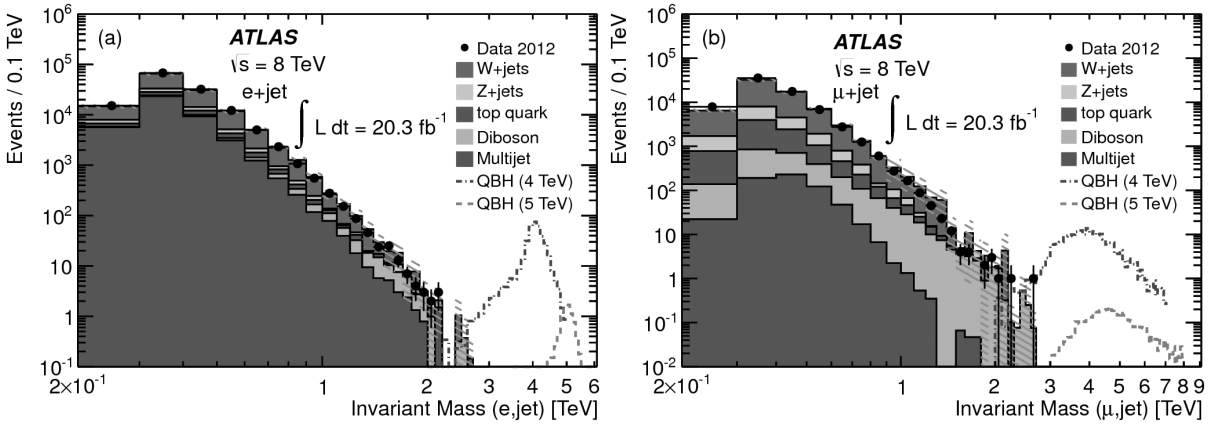

FIGURE 1. The distribution of events over the invariant mass of the lepton and highest-p_T jet for data (points with error bars) and for SM backgrounds (solid histograms). Two examples of QBH signals are overlaid here too. The sum of the uncertainties due to the finite MC sample size and from various sources of systematic uncertainty is shown by the hatched area. (a) – the electron+jet channel, (b) – the muon+jet channel. Taken from Ref. [7].

In Table 1 the numbers of expected background (Exp.), observed (Obs.) events and cumulative signal efficiencies (Eff.) are shown [7]. The observed numbers of events and expected total background are in agreement within the total uncertainty. There is no evidence for any excess.

TABLE 1. Numbers of expected background (Exp.) and observed (Obs.) events, along with the cumulative signal efficiencies (Eff.), with uncertainties including both the statistical and systematic components for various values of $M_{\rm th}$. Taken from Ref. [7].

$M_{\rm th}$		Electron+jet			Muon+jet	
TeV	**Obs.**	**Exp.**	**Eff. [%]**	**Obs.**	**Exp.**	**Eff. [%]**
1.0	1200	1210^{+230}_{-220}	57 ± 4	620	550 ± 280	38 ± 4
1.5	100	110 ± 40	57 ± 4	49	65^{+45}_{-40}	36 ± 4
2.0	12	19^{+13}_{-12}	56 ± 4	8	14^{+16}_{-14}	36 ± 4
2.5	0	$5.3^{+4.5}_{-3.9}$	55 ± 4	3	5^{+6}_{-5}	34 ± 4
3.0	0	$1.8^{+1.8}_{-1.6}$	54 ± 4	1	$2.1^{+2.9}_{-2.1}$	34 ± 4
3.5	0	$0.76^{+0.79}_{-0.67}$	54 ± 4	0	$1.0^{+1.6}_{-1.0}$	33 ± 4
4.0	0	$0.35^{+0.38}_{-0.34}$	53 ± 4	0	$0.57^{+0.94}_{-0.57}$	33 ± 5
5.0	0	$0.09^{+0.10}_{-0.09}$	52 ± 4	0	$0.24^{+0.39}_{-0.24}$	32 ± 5
6.0	0	$0.03^{+0.04}_{-0.03}$	52 ± 4	0	$0.13^{+0.22}_{-0.13}$	32 ± 6

The uncertainties of the signal efficiency are associated with the selection cuts on $\Delta\eta$, $\Delta\phi$, $<\eta>$, $m_{\rm inv}$ and isolation. The uncertainties of the background, the detector simulation and luminosity were taken into account as well. The combined uncertainty on the signal efficiency from these sources spans the values from 3.5% at 1 TeV up to 3.9% at 6 TeV for the electron channel and from 3.6% at 1TeV to 5.6% at 6 TeV for the muon channel.

The cumulative efficiency in Table 1 is taken from the signal MC simulation for QBHs with charge of +4/3. The differences in efficiency between the +4/3 charge state and other charged states are substantially smaller than the above uncertainties.

In Figure 2 you can see the combined 95% Confidence Level upper limits on $\sum \sigma_{\rm qq} \times BF_{\rm qq}$ for QBHs decaying to a lepton and jet, as a function of threshold mass [7].

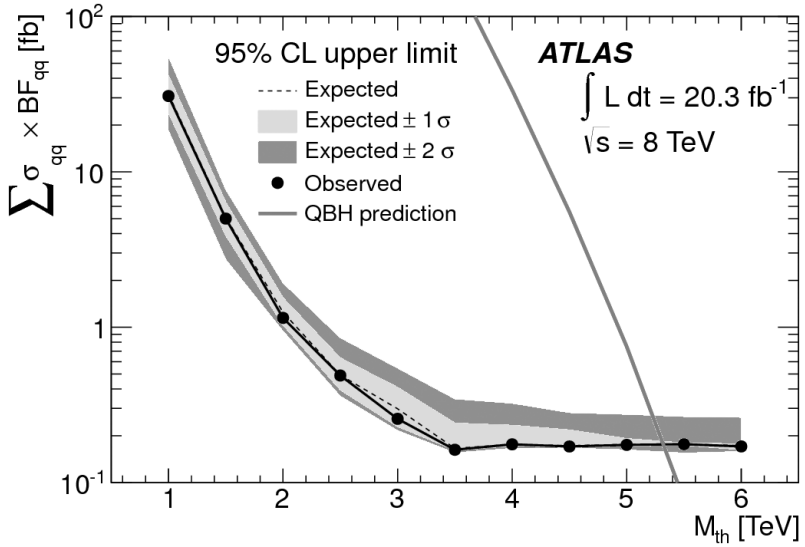

FIGURE 2. The combined 95% CL upper limits on $\sum \sigma_{\rm qq} \times BF_{\rm qq}$ for QBHs decaying to a lepton and jet, as a function of $M_{\rm th}$, assuming $M_{\rm D} = M_{\rm th}$ and $n = 6$ ADD extra dimensions. The limits take into account statistical and systematic uncertainties. Points along the solid black line indicate the mass of the signal where the limit is computed. The $\pm 1\sigma$ and $\pm 2\sigma$ bands indicating the underlying distribution of possible limit outcomes under the background-only hypothesis are also shown. The predicted cross section for QBHs is shown as the solid curve. Taken from Ref. [7].

In this case the multidimensional mass is equal to threshold mass and the number of extra dimensions in the ADD-model is equal $n = 6$. To extract the upper limit on the lepton+jet cross section, a fit to the invariant-mass distribution is performed, replacing the uncertainties due to MC sample size by the statistical uncertainties on the fit parameters. The used CLs method is designed to give conservative limits in cases, where the observed background fluctuates below the expected values. Upper limits on $\sum \sigma_{qq} \times BF_{qq}$ for the production of QBH above M_{th} are determined in the interval 1-6 TeV.

The statistical combination of the channels uses a likelihood function constructed as the product of terms of the Poisson probability, which are describing the total number of events observed in each channel. The systematic uncertainties are included as noise parameters into the likelihood through their effect on the average of the Poisson function. Furthermore, they are also included by convolutions with the Gaussian distributions.

The observed and expected upper limit values are equal to 0.18 fb above 3.5 TeV due to insufficient statistics. The 95% C.L. lower limit on M_{th} is 5.3 TeV.

CONCLUSIONS

In conclusion, a first search for two body lepton+jet final states with a large invariant mass has been performed using 20.3 ± 0.6 fb^{-1} of pp collisions recorded at $\sqrt{s} = 8$ TeV with the ATLAS detector at the LHC. In the invariant mass region above 1 TeV the observed events are consistent with extrapolated background from the low-invariant-mass control region. Above 3.5 TeV the expected background drops below one event and the 95% C.L. upper limit on the electron (muon)+jet $\sum \sigma_{qq} \times BF_{qq}$ is 0.27 (0.49) fb, and the lower limit on M_{th} is 5.2 (5.1) TeV. Assuming lepton universality, the 95% C.L. upper limit on the sum of the product of the QBH production cross sections and branching fractions of decay to lepton+jet is 0.18 fb. The 95% C.L. lower limit on M_{th} is 5.3 TeV.

ACKNOWLEDGMENTS

We thank CERN for the very successful operation of the LHC, as well as the support staff from our institutions without whom ATLAS could not be operated efficiently and members of the Exotics working group for careful analysis and fruitful discussions.

REFERENCES

[1] N. Arkani-Hamed, S. Dimopoulos, and G. R. Dvali, Phys. Lett. B **429**, p. 263 (1998).
[2] I. Antoniadis, N. Arkani-Hamed, S. Dimopoulos, and G. R. Dvali, Phys. Lett. B **436**, p. 257 (1998).
[3] N. Arkani-Hamed, S. Dimopoulos, and G. R. Dvali, Phys. Rev. D **59**, p. 086004 (1999).
[4] D. M. Gingrich, J. Phys. G **37**, p. 105008 (2010).
[5] L. A. Anchordoqui, J. L. Feng, H. Goldberg, and A. D. Shapere, Phys. Rev. D **65**, p. 124027 (2002).
[6] The ATLAS Collaboration, JINST **3**, p. S08003 (2008).
[7] The ATLAS Collaboration, Phys. Rev. Lett. **112**, p. 091804 (2014).
[8] The GEANT4 Collaboration, Nucl. Instrum. Methods Phys. Res. **Sect. A 506**, p. 250 (2003).